Aeroheating Model Advancements Featuring Electroless Metallic Plating

C.J. Stalmach Jr.*
Vought Corporation, Dallas, Texas
and
W.D. Goodrich†
NASA Johnson Space Center, Houston, Texas

Discussed are advancements in wind-tunnel model construction methods and hypersonic test data demonstrating the methods. The general objective was to develop model fabrication methods for improved heat-transfer measuring capability at lower model cost. A plated slab model approach was evaluated with cast models containing constantan wires that formed single-wire-to-plate surface thermocouple junctions with a seamless skin of electroless nickel alloy. Heat-transfer data were obtained from surface-temperature measurements and semi-infinite slab theory. Mach 7 test results obtained using several simple models demonstrated that this plated slab approach provides valid aeroheating data. The materials used in these prototype models limited surface temperature to 550°F.

Nomenclature

A	= area
b	= thickness of metallic skin
erfc	= complementary error function, $(2/\sqrt{\pi})\int_{\beta}^{\infty} e^{-\lambda^2}\,d\lambda$
C, Cp	= specific heat at constant pressure
h	= aerodynamic heat-transfer coefficient
k, K	= thermal conductivity
L	= model length
M	= freestream Mach number
P	= pressure
$\dot{q}$	= heat-transfer rate
R	= radius, or freestream Reynolds number
S	= surface distance
T	= temperature
$\overline{T}$	$= (T_w - T_i)/(T_{aw} - T_i)$
t	= time
x	= axial distance from nose
α	= angle of attack
β	$= h\sqrt{t}/\sqrt{\rho CK}$
λ	= dummy variable of integration
ρ	= density

Subscripts

aw	= adiabatic wall
i	= initial
p	= plate
ref	= stagnation value for sphere (1 ft × model scale)
T	= total
s	= model stagnation
w	= wall

Introduction

AERODYNAMIC testing technology currently plays a major role in establishing data to support vehicle design and to help define trajectories and operational constraints for the Space Shuttle Program. Specifically, predicting the aerodynamically induced forces and surface heat-transfer rates that will be experienced during the atmospheric flight phases of the shuttle mission profile relies heavily on using hypersonic wind tunnels for simulating the flowfield around accurately constructed models of the shuttle launch and entry (orbiter) configurations. This paper includes a description and evaluation of recent advances in wind-tunnel model construction methods applying electroless metallic plating technology. Additional descriptions and applications of these methods are available in Refs. 1 and 2. The general objective of the study reported herein was to develop methods of building wind-tunnel heat-transfer models that had improved measuring capability and accuracy and lower cost compared to more conventional fabrication methods.

A key process to the fabrication approaches was electroless deposition of a metallic alloy to form a seamless model skin. Electroless plating is a means of depositing metal through controlled autocatalytic chemical reduction. An electroless deposition of metal was discovered in 1844 by Wrentz. Improvements (resulting in a patent) were accomplished by Roux in 1916; however, the process was not practical until about 1946 when Brenner and Riddell developed a controllable autocatalytic reduction process.[3-5] Since electrical current is not involved in the deposition, the surface of nonconductors such as plastics may be plated by seeding the surface with a catalyst, generally palladium. The growth of the deposit originates from multitudinous point sources (catalytic centers) on the surface. On a properly prepared surface, the number of nuclei is so large that growth proceeds as a plane front parallel to the original surface. Thus electroless plating produces a plate of uniform thickness wherever the solution may reach, including blind holes and sharp corners (problem areas in conventional electroplating). Most of the electroless nickel alloys contain phosphorous, which results in a very hard plate, comparable to chrome. The nickel phosphorous alloy has very low thermal conductivity, which can be used to great advantage in models that have high surface-temperature gradients. Shipley Company, in its Niculoy 22, improved the ductility of the alloy while retaining hardness with the addition of 1% copper.

An outstanding feature discovered during this study is that a high output, repeatable thermocouple junction resulted when electroless alloy (Niculoy 22) was plated to a single (constantan) wire. The single-wire-to-plate junction greatly

Presented at the AIAA 9th Aerodynamic Testing Conference, Arlington, Texas, June 7-9, 1976; submitted July 18, 1976; revision received May 13, 1977.

Index categories: Testing, Flight and Ground; Boundary Layers and Convective Heat Transfer—Laminar; Boundary Layers and Convective Heat Transfer—Turbulent.

*Senior Engineer. Member AIAA.

†Senior Engineer. Member AIAA.

improved the accuracy and reduced the cost of instrumentation. Major reasons for the improved accuracy are the precision possible in locating each of the one-wire thermocouples and in the reliable and continuous measurement of temperature on the model surface with measured material properties. Plastic casting and electroless plating are low-cost fabrication techniques (after proper facilities and techniques are developed). In addition, the described instrumented-model method is low in cost because the junctions of the wires and plates are formed automatically during the plating process.

This paper identifies several model/instrument fabrication ideas employing electroless plating. A plated slab approach was chosen for laboratory and wind-tunnel evaluations and is the process described in detail.

Technical Objective

The objective of this effort was to develop new techniques for fabricating aeroheating models that incorporate as many of the following characteristics as possible: 1) minimum of surface joints, 2) close reproduction of surface contours, 3) smooth surface finish suitable for boundary-layer transition studies, 4) surface heat sensors that can be predictably located, 5) hard surfaces that have good resistance to abrasion by particles, 6) structural strength sufficient to withstand hypersonic flows at high dynamic pressures, 7) high sensor sensitivity or means of tailoring the sensitivity to the model location and the facility conditions, 8) instrument placement permitted anywhere on the model surface, 9) effective measurement of heat transfer in areas of high-temperature gradients, and 10) fabrication time and cost less than conventional machining methods.

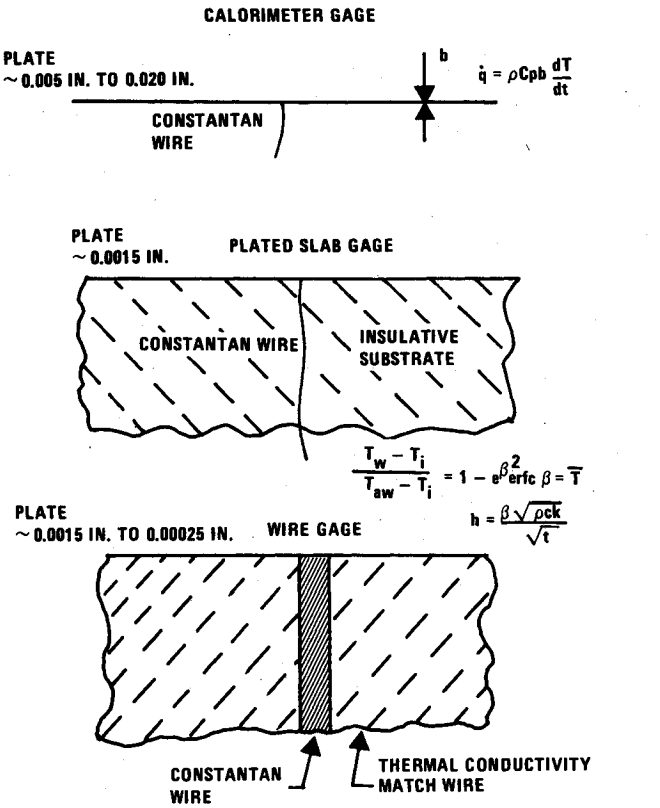

Fig. 1 Model/instrumentation concepts employing electroless nickel skin.

Model Development Program

Development of improved model methods included a review of past experiences in the literature and heating analysis to help screen a list of promising concepts. A plated-slab method was chosen for laboratory development based on analyses, previous experience and cost considerations. After evaluating several fabrication procedures, sample models were made and evaluated in a hypersonic wind tunnel where validation of the approach was achieved.

Trade Studies

A literature search was conducted[6] for the following subjects: electroless plating of plastics, casting of wind-tunnel models, and heat-transfer measurements. Heat-transfer measurement techniques considered for application of electroless plating and single-wire-to-plate thermocouples included the calorimeter, the Gardon gage, and the semi-infinite slab.

Figure 1 shows examples of employing electroless nickel to form a seamless skin that is an integral part of the instrumentation. In all of these approaches, electroless nickel (Niculoy 22) was plated to constantan wire. This procedure provided an excellent thermocouple, comparable to copper/constantan as shown in Fig. 2.

A calorimeter skin formed by the electroless method (Fig. 1) has advantages when compared with machining or electroforming that include the following: 1) plating is to one-wire rather than welding of two wires, 2) it is seamless over the total surface, and 3) it has uniform plate thickness (inherent for electroless, difficult in electroplating and machining), 4) harder surface, and 5) lower thermal conductivity. As an example fabrication approach,[6] a replica of a model was cast with a low-melting-temperature alloy (Cerrotru, a product of Cerro de Pasco Corporation). After plating, the replica was melted and removed, leaving a free-standing shell. If the casting had included the thermocouple wires and sting/model adapter, they would have been joined to the skin during the plating operation.

A Gardon gage[7] is a steady-state instrument that obtains heat transfer from measurements of the delta temperature from the center of a thin disk to its outer edge. The disk edge is cooled by a heat sink. A means of plating a free-standing, instrumented disk for a Gargon gage is similar to that described for the calorimeter gage.[6]

Two classes of semi-infinite slab techniques incorporating electroless plating are shown in Fig. 1. Heat transfer is obtained from measurement of the surface temperature, knowledge (from calibrations) of the material properties, and application of semi-infinite slab heating theory. A plated slab model makes use of an insulative casting, similar to that used in the phase-change paint method.[8] The surface-temperature distribution, however, is measured continuously with thermocouples in the plated slab method. The approach will be discussed later in detail.

Variations in material property have been experienced when fillers are used in epoxy castings,[9] whereas the thermal properties are known and repeatable for thermocouple wire. The wire-gage concept (Fig. 1) takes advantage of these facts. Use of a substrate that has thermal properties very similar to the wire is required. Electroless nickel plating of the surface forms the thermocouple junction. A wire gage inserted in a steel model is similar in concept to the coaxial gage.[10] The wire gage has the advantages of requiring only one thermocouple wire per junction and exhibiting a continuous surface.

An analytic program was conducted to assess the effects of the geometric and thermal property variations on the design and accuracy of the various model/instrument concepts. The input heating condition represented a flow condition in the NASA Ames 3.5-ft hypersonic wind tunnel for a 1-in. diameter hemisphere that represented the model size chosen for the Phase A test. Figure 3 shows effects of wire and plate dimensions for Emerson Cuming's Stycast 2762FT. The plate thickness (0.001-in.) and wire diameter (0.003-in.) provided reasonable temperature histories for a plated slab model in the selected facility. Large wire diameters (0.032-in.) approached

a semi-infinite wire gage response for the insulative substrate if the Niculoy plate was sufficiently thin (0.00025 in.). Further results of the analysis and description of the computer program are discussed in Ref. 6.

Plated Slab Technique

The plated slab model technique was chosen during the trade studies as the most worthy of further development. The summarized fabrication steps for a plated slab model are as follows:

1) The model was cast to the final external geometry using an insulative, high-temperature material.

2) Prior to casting the model, thermocouple wires were positioned into accurately located holes in the mold. (The holes were developed during the mold-casting operation.) The resultant model exhibited a thermocouple wire protruding the surface at each sensing location.

3) An electroless metallic plate was deposited over the external model surface in two coats; the thermocouple wires were polished flush to the plated surface after the first coat.

The geometrically accurate models had a seamless metallic skin with single-wire-to-plate thermocouple junctions that provided surface-temperature measurements.

The development program sought an optimum combination of commercially available materials for the casting, plate, and wire. The specific plate and wire materials were chosen early in the program when it was demonstrated that Niculoy 22 electroless nickel alloy forms a suitable thermocouple junction with constantan (Fig. 2). The major task, then, was to evaluate casting materials in regard to achieving the program objectives and maximum compatibility with a selected plating process. Materials that passed literature and analytic screening and that were evaluated in the laboratory are listed in Table 1. The hydraulic setting refractories did not provide the desired surface finish. Initial processes‡ for plating-to-plastics did not provide satisfactory results with the high temperature epoxy materials of Table 1.[6]

The kernel of the development was customizing the casting material and preplating process. An innovative procedure that provided the first acceptable model was an aluminum transfer process referred to as ATZN.§ The aluminum-transfer method provided a very thin film of aluminum powder that was bonded to the epoxy surface during the casting operation.[6] The electroless plate adhered tightly to the bonded aluminum resulting in moderately high-temperature resistance of the plate/substrate interface. Since surface etching was not involved, the plated surface exhibited excellent surface smoothness.

Table 1 Casting materials (and fillers) evaluated in the plated slab approach

Casting material (trade name and no.)	Epoxy filler material
Hydraulic setting refractories	Short Fibers
LO-XA125	Glass
Thermo-Sil 120	PVA
Kaolite 2200	Powders
High-temperature epoxies	Quartz
Stycast 2762FT	Graphite
3070	Boron nitride
1095	Calcium carbonate
2850KT	Aluminum
Novimide 700/55	Copper
Epocast 21	Carbolized iron
Shell 828	Pure iron
Dow 438	
431	

‡SSPN: Sensitized Smooth Plastics Nickel Plate.

§ATZN: Aluminum Transfer Zinc-Aid Nickel Plate.

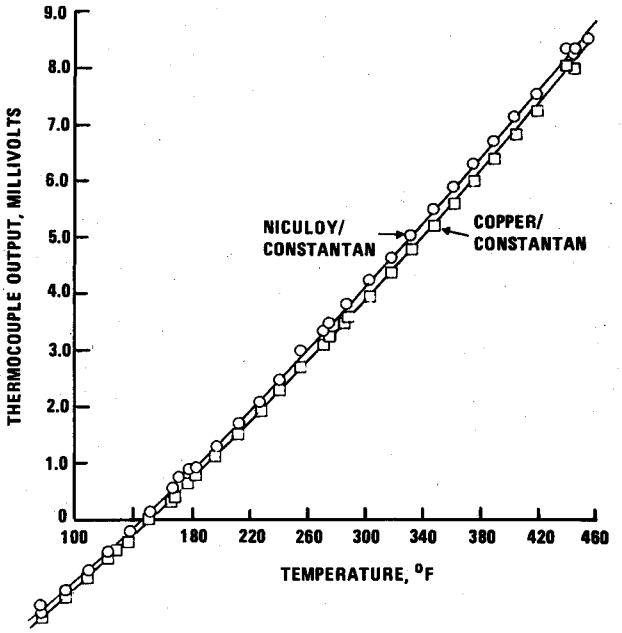

Fig. 2 Calibration of Niculoy/constantan and copper/constantan thermocouples.

Smooth nickel and copper electroless platings were achieved with the aluminum-transfer process for several epoxy materials. Oven tests demonstrated, however, that the temperature resistance of the plate-to-epoxy bond was sensitive to the material composition and preplate process. The material should have a coefficient of thermal expansion near that of the plate and bond well to the aluminum powder (without wetting the outer aluminum surface). Stycast 3070 with 4% (by weight) powdered graphite provided the best results of the materials evaluated for the ATZN process.[6] This material with the best of the preplate processes evaluated resulted in substrate/plate interface bonds that would normally survive 350°F in oven tests. An increase in temperature service is considered possible with additional material/process development.

Another acceptable process developed for a plated slab model was designated as ECAN.¶ This development (in cooperation with Shipley Company) refined the approach of preplate etching of plastics to better condition the surface prior to the sensitizing step. The mechanical strength of the plate attachment to a plastic is greatly increased if the surface is slightly porous to permit the plate to mechanically latch into these pores. Materials developed for plated plastics in industry do not have the temperature resistance required in this study. High-temperature epoxies do not etch readily and generally develop a rough, pitted, or grainy surface rather than the tiny, contorted tunnels desired. It was discovered, however, that an etched surface of Stycast 3070 was more suitable for plating than normally considered for epoxies, possibly explained by the calcium carbonate powder filler contained in this material. Calcium carbonate reached by an acid dissolved, leaving random, fine-grain voids in the epoxy surface. Oven evaluation demonstrated that the ECAN process would permit plated Stycast 3070 or Stycast 3070 with 4% glass fibers to withstand temperatures up to 550°F. This exceeds the maximum temperature quoted for the epoxy material. The surface finish was improved with the glass filler; however, none of the ECAN models possessed surfaces as smooth as the ATZN models. Details of the ECAN process are discussed in Ref. 6.

¶ECAN: Etch, Catalyst, Accelerator, Nickel Plate.

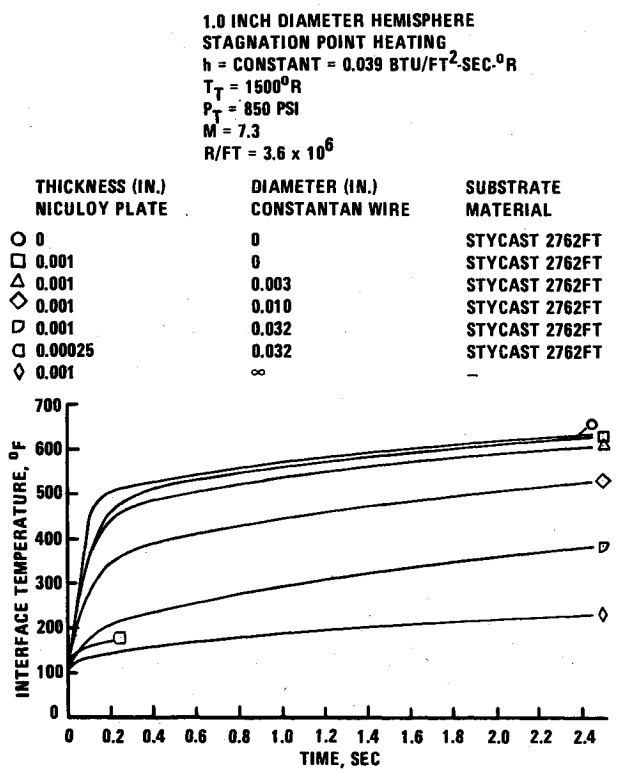

Fig. 3 Temperature response of Niculoy-plated Stycast 2762FT, effects of wire and plate dimensions.

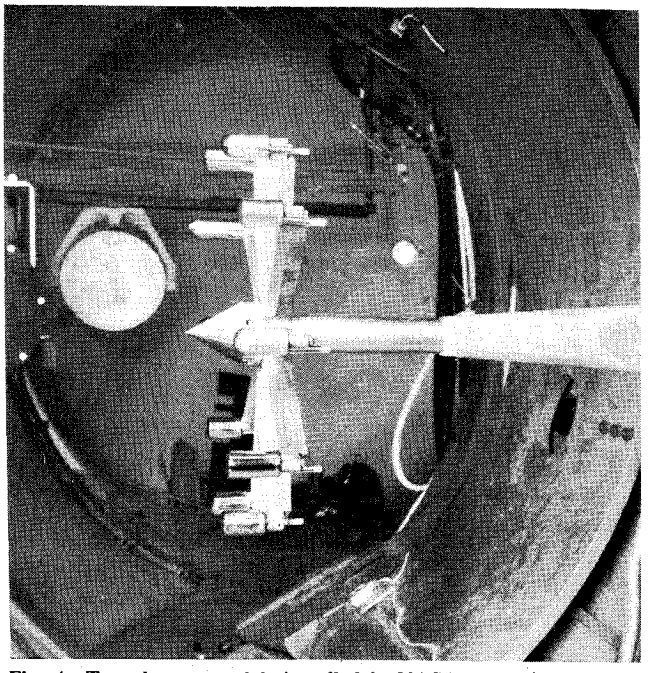

Fig. 4 Ten phase-a models installed in NASA Ames 3.5-ft hypersonic wind tunnel.

Wind-Tunnel Evaluation of Plated Slab

Two simple model geometries shown in Fig. 4 were tested at $M=7.3$ in the NASA Ames 3.5-ft hypersonic wind tunnel. The hemisphere cylinder provided ease of comparison to existing data and theory. The flat face cylinder geometry provided a good assessment of the instrumentation accuracy in areas of high-surface-temperature gradients and assessment of the particle resistance of the plate. Two master models (machined thin-skin calorimeters) and eight plated slab models were tested simultaneously by using the mount shown in Fig. 4. Eight runs were conducted at $M=7.3$ at a nominal total temperature of 1500°R. The test began at Reynolds number 0.8×10^6 per ft and progressed to 4.0×10^6 per ft. The models were inserted into the flow stream for about 2 sec. Thermocouple outputs from the models were digitized and recorded on magnetic tape.

The data reduction procedure applied for this initial demonstration of the plated slab model made use of the semi-infinite slab solution as expressed by Jones and Hunt[8]:

$$\bar{T}=1-e^{\beta^2}\,\mathrm{erfc}\beta$$

$$\bar{T}=(T_w-T_i)/(T_{aw}-T_i)$$

$$\beta=h\sqrt{t}/\sqrt{\rho CK}$$

This procedure assumes a one-dimensional, homogeneous material with known thermodynamic property. Heat film coefficients, however, were successfully calculated at specific times during a run using these equations by combining the three elements of material (substrate, plate, and wire) into one equivalent material property term $\sqrt{\rho CK}$ and permitting this term to vary with time. The equivalent material property term $\sqrt{\rho CK}$ was determined with a plated slab hemisphere cylinder model (known h) through testing in the wind tunnel. This hemisphere (calibration) model was tested simultaneously with the plated slab flat face cylinder models that represented the test models for which h was to be determined. The above set of equations[8] was used to determine $\sqrt{\rho CK}=f(\sqrt{t})$ from the measured temperature time histories (Fig. 5, for example) and known value of h for specific locations around the hemisphere model. The same set of equations was then used to calculate h for the flat face models from the temperature time histories measured with those models and the calibrated, time-dependent material property. The analytic program (Fig. 3) had indicated that for the wire diameter (0.003 in.) and plate thickness (0.0015 in.) of this study the time history of the surface temperature for an instrumented plated slab was close to the surface temperature of an assumed homogeneous insulative material (Stycast). Most of the temperature difference (Fig. 3) occurred in the initial half second of a tunnel run. The effects of the plate and the thermocouple wire on the in-depth heating of the substrate, therefore, were lumped into the equivalent material property term $\sqrt{\rho CK}=f(\sqrt{t})$ with the results shown in Fig. 6. The relation of $\sqrt{\rho CK}$ to $\sqrt{t}$ was suggested by Ref. 9 and the slope of the data in Fig. 6 at time 1 sec (where the influence of the wire and plate is small) is similar to that of Ref. 9 for a substrate material only (Stycast 2762). The heat film coefficient h was calculated for several selected times between the interval 0.1-1.75 sec using the time-dependent model surface temperature and equivalent material property data. As expected, the value of h was found to be constant for a given model location and for a given test condition. This fact helped justify the simplification of combining the wire, plate, and substrate effects into one equivalent material term.

The stepwise procedure used in determining the unknown parameter h for the models is outlined (for clarity):

1) Measure and plot temperature-time data for all plastic models.

2) Determine the effective time zero (t_i) and initial wall temperature (T_{wi}) (Fig. 5).

3) Calculate $\bar{T}$ at selected times.

4) Determine β from $\bar{T}$ (Ref. 8).

5) Establish distribution of h for a hemisphere for the subject test condition. (In this test the distribution of h was measured with a thin skin calorimeter model.)

6) Calculate $\sqrt{\rho CK}$ at each model station and time for the plastic hemisphere models by using the known values of h.

7) Plot $\sqrt{\rho CK}$ as a function of $\sqrt{t}$ for all model positions, all times and all runs for given materials on a hemisphere model (Fig. 6).

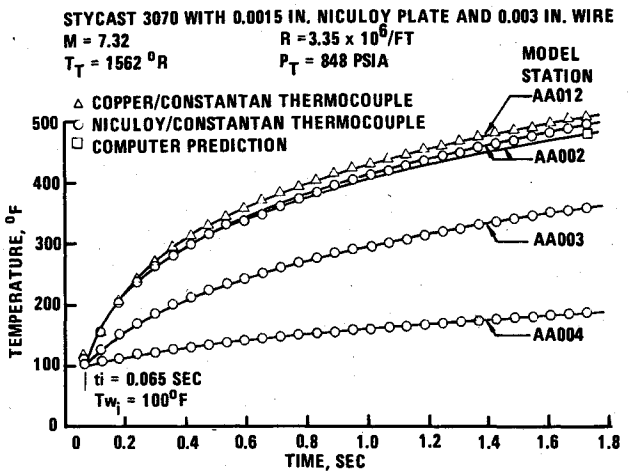

Fig. 5 Temperature history of model AA hemisphere, run 5.

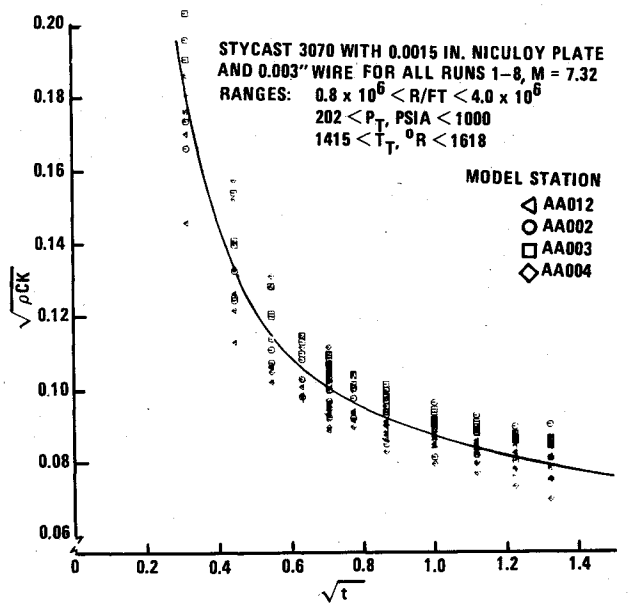

Fig. 6 Material property of model AA hemisphere.

8) Calculate h for the flat face plastic models for several values of time at each model station using the faired plot of $\sqrt{\rho CK}$ determined from a hemisphere model that was composed of the same materials.

9) Plot averaged values of h as a function of model location (Fig. 7).

The heating distribution for the plastic flat-faced models (two different plating processes) compared well with that of the master, thin-skin calorimeter model data, and previous experience[11] as shown in Fig. 7. The averaged stagnation heating measured by the master flat-face model was 1% higher than that predicted by the theory of Zoby-Sullivan.[12] The averaged stagnation heating for the hemisphere master model was 2% higher than the theory of Fay-Riddell (as provided by the NASA Ames data reduction routine). As noted in Fig. 8, the surface resulting with the ECAN process (Model CC) was much rougher compared to the ATZN process (Models G and I). The ATZN models generally failed after one or two runs under these test conditions, however.

The sensitivity of the fairing of the equivalent material term $\sqrt{\rho CK}$ on the calculation of h was examined. Calculations of h for one of the models (Model CC) were made for a lowermost fairing of Fig. 6 and the heating results were 8% lower.[6] The data in Fig. 6 did not distinguish any dependency on the local model geometry (model station). The increasing value for $\sqrt{\rho CK}$ as time approaches zero in Fig. 6 is

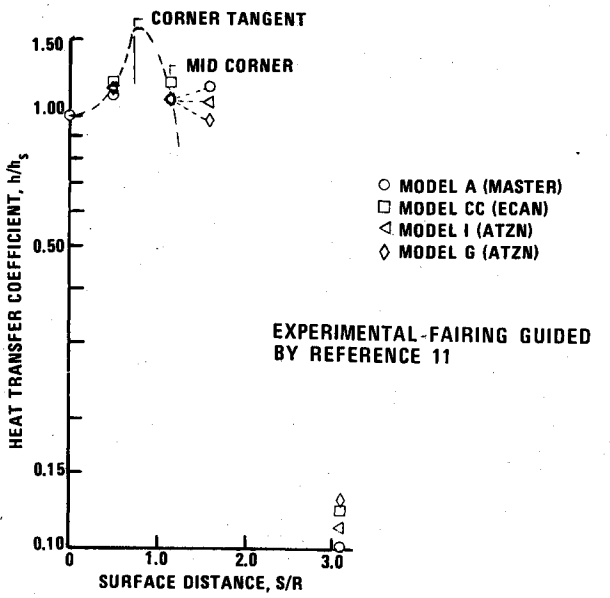

Fig. 7 Distribution of film coefficient on flat-faced cylinder, $M = 7.32$.

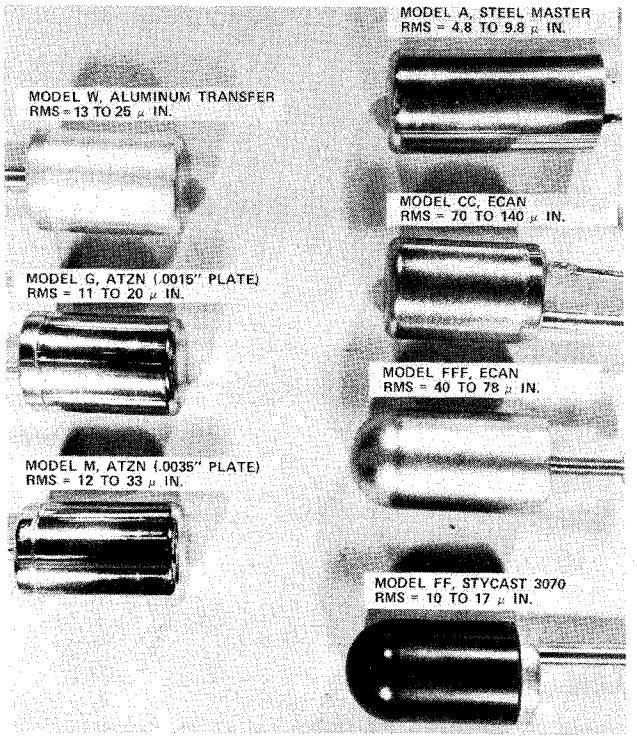

Fig. 8 Representative development models.

attributed to the inclusion of the influence of the wire and plate into this term (review also Fig. 3). As mentioned (in the data reduction of the tunnel test) combining the wire, plate, and substrate properties in the $\sqrt{\rho CK}$ term did not cause any time dependency in the calculated values of the film coefficient h. Further proof of the validity of this data procedure was indicated through the good agreement of the computer-predicted model surface temperature to the wind-tunnel-measured temperature histories as shown in Fig. 5. For this comparison, the computer routine was given constant values for h, $\sqrt{\rho CK}$ for the plastic substrate, $\sqrt{\rho CK}$ for the wire, and $\sqrt{\rho CK}$ for the plate. Material property values for the wire and the plate were obtained from the literature. A constant value of $\sqrt{\rho CK}$ for the plastic was based on the wind-tunnel experiment by taking the value at time 1 sec from Fig. 6 where

the influences of the wire and plate are considered negligible. The experimental value of h was used. The influences of the wire and plate on the predicted temperature time history were taken into account in the computer routine through thermal balance of the finite elements of the three materials for each finite step in time.

Figure 5 indicates agreement in temperature measurements between the new Niculoy/constantan and standard copper/constantan thermocouples for ECAN Model AA. (Model stations 012 and 002 are equal distance from stagnation point.) The temperature agreement was even better for the smoother models.[6]

Combined laboratory and tunnel results demonstrated that the plated slab concept can provide the following stated program objectives: 1) no surface joints, 2) good surface detail reproduction, 4) accurate instrument location, 6) sufficient strength, 8) instrument placement anywhere, 9) effectiveness in areas of high thermal gradients is equal to other semi-infinite slab approaches.

The plated slab possesses a very hard surface that is resistant to particle damage and therefore meets in principle the model objective 5. Particle damage of the models did occur in the pebble-bed heater facility used in this evaluation. Post-test magnified views,[6] however, indicated that particle damage resistance of the ECAN models was comparable to a heat-treated stainless steel model. Electroless copper-plated models had more severe particle damage.

The customization of sensor sensitivity, objective 7, was restricted to materials that provided good plate-to-substrate bond strength. The best materials for bond strength fortunately also provided good data sensitivity.

These tunnel results demonstrated that this model method will provide accurate data. Further improvements in accuracy can be expected as material, process and data reduction improvements are made. The Niculoy/constantan thermocouple greatly enhanced the overall attractiveness of this modeling approach. The principal problem area was finding an acceptable compromise between surface smoothness, plate hardness, and maximum operation temperature of the model.

The photograph of Fig. 8 provides representative surface smoothness measurements of master, ATZN, and ECAN models. The smoothness of ATZN models are considered adequate for applications involving natural hypersonic boundary-layer transition (objective 3). Polishing marks of the master were reproduced in the plated plastic models,[6] which attested to the faithful reproduction of surface detail of this process.

The ATZN process in the current state of development is restricted to maximum temperature of approximately 300-350 °F. The ATZN models generally fail in the cool-down process when the compressive stress in the plate overcomes the bond strength of the plate. The compressive stress is attributed to the deposition process and from the difference in coefficient of thermal expansion of the plate and substrate.

Electroless copper used with aluminum transfer method (ATZC) met both the temperature and surface smoothness requirements. Such a model survived all eight runs at stagnation temperature exceeding 650°F without a temperature induced failure. The bond strength of the electroless copper is not considered to be higher than electroless nickel; therefore the lack of wrinkling is assumed to mean lower plating, and thermal expansion stresses exist at the interface. The copper skin, however, is poor in particle resistance compared to the nickel alloy.

Model CC represents the highest roughness of the ECAN models, and Model FFF represents the best surface finish obtained for the ECAN process (Fig. 8). The ECAN models survived, in general, all eight runs at stagnation-point temperatures exceeding 650°F. Oven tests (where the models were heat soaked and cooled) generally caused local plate blistering in ECAN models when cooling from 550°F. Therefore, the ECAN demonstrated operating temperatures exceeding the rated temperature of the plastic substrate.

Models AA and CC provided valid heating data for the model geometries of this study (Figs. 6, 7) even with undesirable roughness. The improved surface finish of ECAN (Model FFF) should prove adequate for many model applications.

Applications and Future Developments

The plated-slab model approach, including the innovative single-wire-to-plate thermocouple instrumentation is most applicable to complex geometries where numerous heat-transfer sensors and a seamless skin are required. The reported state of development limits the maximum plate/substrate interface temperature to (about) 550°F for the ECAN and 350°F for the ATZN process. These temperature limits are adequate for most lee-side measurements, whereas restrictions in exposure time of the model or enthalpy of the flow may be necessary for windward testing applications. Material and process development should continue so that the full potential of the plated-slab concept will be realized.

Other model approaches (Fig. 1 and Ref. 6) possess attractive potential and deserve further development.

Conclusions

A plated-slab heat-transfer model concept that incorporated single-wire-to-plate thermocouples was developed and the approach demonstrated in a wind-tunnel test. This model construction method provides a means of obtaining multitudinous heat-transfer measurements along any surface geometry without seams in the model surface.

Acknowledgment

This research and development effort and other related developments[1,2,6] were supported by NASA Johnson Space Center under Contract NAS9-13692 to Vought Corporation and interagency test arrangements with NASA ARC and AF AEDC.

References

[1] Stalmach, C.J. and Goodrich, W.D., "Aeroheating Model Advancements Featuring Electroless Metallic Plating," *Proceedings of AIAA 9th Aerodynamic Testing Conference,* June 1976.

[2] Goodrich, W.D. and Stalmach, C.J., "Effects of Scaled Heat-shield Tile Misalignment on Orbiter Boundary Layer Transition," *Journal of Spacecraft and Rockets,* Vol. 14, Oct. 1977, pp. 638-640.

[3] Brenner, A., "History of the Electroless Plating Process," ASTM STP No. 265, 1959, pp. 1-2.

[4] Gorbunova, K.M. and Nikiforova, A.A., "Physicochemical Principles of Nickel Plating," National Science Foundation TT63-11003, 1963, translated from Institute of Physiochemical, Academy of Science of the U.S.S.R., 1960.

[5] Goldie, W., "Metallic Coating of Plastics," Electrochemical Publication, Ltd., Middlesex, England, Vol. 1, 1968.

[6] Stalmach, C.J., "Developments in Convective Heat Transfer Models Featuring Seamless and Selected-Detail Surfaces, Employing Electroless Plating," Vought Corporation, Dallas, Texas, TR2-57110/5R-3227, June 1975; also NASA CR 144364.

[7] Gardon, R., "An Instrument for the Direct Measurement of Intense Thermal Radiation," *Review of Scientific Instruments,* Vol. 24, May 1953, pp. 366-370.

[8] Jones, R.A. and Hunt, J.L., "Use of Fusible Temperature Indicators for Obtaining Quantitative Aerodynamic Heat-Transfer Data," NASA TR-R-230, Feb. 1966.

[9] Matthews, R.K., Eaves, R.H. Jr. and Martindale, W.R., "Heat-Transfer and Flow-Field Tests of the McDonnell Douglas-Martin Marietta Space Shuttle Configurations," AF AEDC-TR-73-53, April 1973.

[10] Trimmer, L.L., Matthews, R.K., and Buchanan, T.P., "Measurement of Aerodynamic Heat Rates at the Von Karman Facility," International Congress on Instrumentation in Aerospace Simulation Facilities, Sept. 1973.

[11] Jones, R.A., "Heat-Transfer and Pressure Distributions on a Flat-Face Rounded-Corner Body of Revolution With and Without a Flap at a Mach Number of 8," NASA TMX-703, Sept. 1962.

[12] Zoby, E.V. and Sullivan, E.M., "Effects of Corner Radius on Stagnation Point Velocity Gradients on Blunt Axisymmetric Bodies," NASA TM X-1067, March 1965.